Wind error comparison of four different wavelengths of Nd:YAG laser

Heyong Zhang (张合勇)*, Deming Ren (任德明), Weijiang Zhao (赵卫疆), and Yanchen Qu (曲彦臣)

Department of Optic-Electronics Information Science and Technology, Harbin Institute of Technology, Harbin 150080, China

**E-mail: yonghezhang1116@126.com*

Received July 17, 2008

The wind error of multichannel lidar system is simulated through calculation of atmospheric back-sacttering echo signal and weighted least-square fitting. By comparing the wind errors of four wavelengths of the Nd:YAG laser, two kinds of phenomena are found: when the wavelength is 1064 nm, the wind error is the smallest at all different heights; with the aerosol-molecular ratio descending and finally tending to 1, the statistic error increases sharply, which shows that low aerosol-molecular ratio is quite disadvantageous whatever the signal intensity is.

OCIS codes: 010.0010, 010.1100, 010.1290.
doi: 10.3788/COL20090705.0364.

Global wind measurements are required to better understand and forecast weather. Active remote sensing methods, particularly lidar methods, have demonstrated their ability to provide wind measurements throughout the atmosphere from ground-based and airborne platforms[1]. Doppler lidar systems fall into two categories: coherent detection and direct-detection systems. Coherent detection is a heterodyning technique that mixes the echo signal with a second laser beam, often a local oscillation with an offset in frequency, to produce a beat frequency that is related to the Doppler shift. Coherent lidars, which have been developed and used for many years, operate in the infrared (IR) and near-IR wavelength regions. Direct-detection systems rely on directly sensing the wavelength shift of the return signal using a spectral resolving analyzer. In contrast to coherent lidars, the direct-detection systems tend to operate at shorter wavelengths. There are two direct-detection Doppler lidar techniques: edge technique (EDG) and multichannel (MC) technique[2,3]. There has been a report on the Atmospheric Laser Doppler Instrument (ALADIN) designed by the European Space Agency[4], which can measure the wind speeds from the ground up to 30-km altitude with a vertical resolution ranging from 0.5 to 2 km. The resolution steps can be modified during flight and independently for the two measurement channels of the instrument operating on the molecule (Rayleigh) channel and aerosol (Mie) channel. The aerosol ("Mie") receiver is based on a Fizeau interferometer. The molecule ("Rayleigh") receiver is based on a double-edge sequential Fabry-Perot (F-P) interferometer. ALADIN comprises a high-energy laser and a direct-detection receiver operating on aerosol and molecular backscattering signals in parallel. The laser is all solid-state based on Nd:YAG technology and high-power laser diodes (LDs). The detector is a silicon charge-coupled device (CCD) whose architecture allows on-chip accumulation of the return signals, providing photon counting performance. The 1.5-m-diameter telescope is lightweight, all made of silicon carbide. The design of lidar system based on EDG technique has been introduced by Ma *et al.*[5]. The MC method divides the F-P interferometer output into several "channels" or wavelength intervals to enable full resolution of the spectrum. The signals on each channel are measured simultaneously and independently. The Doppler shift is inferred by comparing the central wavelength of the atmosphere affected spectra with the central wavelength of the outgoing laser. The MC system is capable of measuring Doppler shifts that are very small compared with the instrument resolution. Some researchers have carried out the error analysis for lidar[6,7], but they have not given the error at different wavelengths. At present, there are mainly four kinds of wavelengths for usual Nd:YAG laser, which are 1064, 532, 355, and 266 nm. Wind error is acquired through inversion technique with weighted least-square fitting.

Before the inversion, it is necessary to calculate the echo signal of the lidar through the basic lidar equation[8]:

$$P_{\rm r}(r,v) = \frac{P_{\rm t}O_{\rm T}(r)A_{\rm T}\Delta hT^2(r)}{4\pi r^2} \{P_{\rm A}(\pi,r)\beta_{\rm A}(r) * B_{\rm A} + P_{\rm M}(\pi,r) \beta_{\rm M}(r) * B_{\rm M}\}, \quad (1)$$

where $P_{\rm r}(r,v)$ is the power returned from range r and wave number v, $P_{\rm t}$ is the laser power transmitted to the sky, $O_{\rm T}(r)$ is the fractional overlap of the laser beam and the telescope as a function of range, $A_{\rm T}$ is the area of the telescope, Δh is the length of the range bin over which scattering is returned, $T^2(r)$ is the two-way transmission of the atmosphere to range r, and the r^2 term in the denominator takes into account the drop in flux of backscattered light as a function of range. The term in braces describes the scattering response of the atmosphere to the laser light and has been split into separate aerosol and molecular terms, denoted by the subscripts A and M, respectively; β is the volume scattering coefficient, which describes the average amount of scattering material over the range bin; β is multiplied by the backscattering phase function $P(\pi,r)$ to describe the amount of light scattered

per unit solid angle into the field-of-view from range r, B denotes the broadening effect due to the backscattering in atmosphere, and $*$ denotes convolution. We can deduce the relationship between the phase function and the volume scattering coefficient as[9]

$$P(\theta,\varphi)=4\pi\cdot\frac{\int_{r_1}^{r_2}n(r)\beta^0(\theta,\varphi,r)\mathrm{d}r}{\int_{r_1}^{r_2}n(r)\sigma_{\mathrm{s}}^0(r)\mathrm{d}r},\tag{2}$$

where σ_{s}^0 is the volume scattering coefficient β above, and $\beta^0(\theta,\varphi)$ is the differential coefficient scattering section. So there is no necessary to calculate the phase function and the volume scattering coefficient respectively, $\beta^0(\theta,\varphi)$ can replace both of them. $\beta^0(\theta,\varphi)$ can be expressed as

$$\beta^0(\theta,\varphi)=\left(\frac{\lambda}{2\pi}\right)^2[|s_1(\theta)|^2\sin^2\varphi+|s_2(\theta)|^2\cos^2\varphi].\tag{3}$$

The detailed explanation can be found in Ref. [10]. Considering the multi-particle case in the unit volume, the aerosol distribution model will be used in the form of logarithmic normal distribution[11]:

$$n(r)=\frac{N}{\sqrt{2\pi}\ln\sigma}\exp\left[-\frac{(\ln r-\ln r_{\mathrm{bar}})^2}{2(\ln\sigma)^2}\right],\tag{4}$$

where r_{bar} is the geometrical average radius of the particle system; σ is the geometrical standard deviation; N is the total number of particle in the unit volume, and it is the function of altitude z,

$$N(z)=N_0\times\mathrm{e}^{-z/h_0},\tag{5}$$

where N_0 is aerosol concentration on the sea level, h_0 is the coefficient of altitude z. At this time, the individual broadening terms B_{A} and B_{M} described in Eq. (1) can be neglected. In the course of calculation of $\beta^0(\theta,\varphi)$, the refractive index of aerosol particle will be used.

If we select the parameters shown in Table 1, we can acquire the relationship between the wavelength and the echo signal, which is the basis of the analysis of the errors at the four wavelengths. As shown in Fig. 1, Rayleigh scattering is dominant in the short-wavelength direction, while in the long-wavelength direction, Mie scattering is the leading part. The ratio of the two signals is decisive in the discussion of the errors at the four wavelengths.

The error analysis is based on the MC technique.

Table 1. Parameters in the Numerical Simulation

Parameter	Value
Transmitted Energy $\mathrm{P_t}$	60 mJ/pulse
Pulse Width $\Delta\tau$	40 ns
Light Velocity c	3×10^8 m/s
Aerosol Density N_{A}	1×10^5 cm^{-3}
Molecule Density N_{M}	2.55×10^{19} cm^{-3}
Aerosol Refractive Index m	1.33−0.01i
Atmosphere Refractive Index n	1.0002932
Overlap Coefficient $O_{\mathrm{T}}(r)$	1
Range Bin Length Δh	150 m
Telescope Area A_{T}	1555 cm^2
Detection Distance r	2×10^3 m
Aerosol Radius a	0.01−10 μm

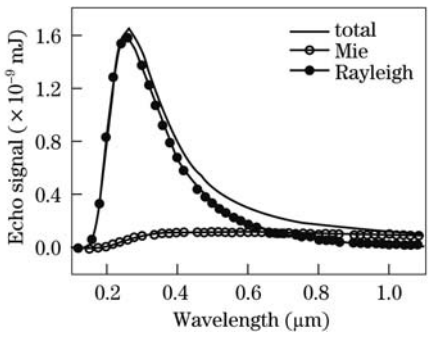

Fig. 1. Echo signal at the altitude of 2 km.

Direct-detection lidar results in two kinds of errors (the statistic error and the system error). The statistic error is dominant so that the system error can be neglected[12]. As for the F-P interferometer, the lidar equation is turned into

$$\begin{aligned}N(r,j) &= \frac{P_{\mathrm{T}}\lambda}{hc}O_{\mathrm{A}}(r)\frac{A_{\mathrm{T}}}{4\pi r^2}\Delta h\frac{Q_E T_0}{n_{\mathrm{C}}}\\ &\quad\sum_{n=0}^{\infty}A_n\cos 2\pi n\left[\frac{j-j_0(r)}{N_{\mathrm{FSR}}}\right]\cdot\mathrm{sinc}\left(\frac{n}{N_{\mathrm{FSR}}}\right)\\ &\quad\exp\left(-\frac{\pi^2n^2\Delta\nu_{\mathrm{L}}^2}{\Delta\nu_{\mathrm{FSR}}^2}\right)\\ &\quad\left[\alpha(r)+\omega(r)\exp\left(-\frac{\pi^2n^2\Delta\nu_{\mathrm{M}}^2}{\Delta\nu_{\mathrm{FSR}}^2}\right)\right],\end{aligned}\tag{6}$$

where j denotes the jth channel of the detector, the subscription FSR represents free spectral range, some other parameters are defined in Table 2, and $\alpha(r)$, $\omega(r)$, and $j_0(r)$ are defined as

$$\begin{aligned}\alpha(r) &= P_{\mathrm{A}}(\pi,r)\beta_{\mathrm{A}}(r)\cdot\\ &\quad\exp\left\{-2\int_0^r[\sigma_{\mathrm{A}}(r')+\sigma_{\mathrm{M}}(r')]\,\mathrm{d}r'\right\}.\end{aligned}\tag{7}$$

$$\begin{aligned}\omega(r) &= P_{\mathrm{M}}(\pi,r)\beta_{\mathrm{M}}(r)\cdot\\ &\quad\exp\left\{-2\int_0^r[\sigma_{\mathrm{A}}(r')+\sigma_{\mathrm{M}}(r')]\,\mathrm{d}r'\right\},\end{aligned}\tag{8}$$

$$j_0(r) = \frac{N_{\mathrm{FSR}}}{\Delta\nu_{\mathrm{FSR}}}\left[(\nu_0-\nu_{\mathrm{c}})-\frac{2U_{\mathrm{H}}(r)\nu_0\sin\phi}{c}\right],\tag{9}$$

where v_{o} is the frequency of the laser, v_{c} is the central frequency of the etalon, U_{H} is a wind componet which will be characterited later. α(r) and ω(r) represent the contribution of aerosol and molecule separately, and $j_o(r)$ is relative to the Doppler frequency shift. Now the main problem is how to inverse $j_0(r)$, $\alpha(r)$, and $\omega(r)$ through the photons detected by the 12 channels. We adopted the weighted least-square fitting. The next step in the inversion process is to linearize Eq. (2). One can accomplish linearization by expanding the relevant variables in a Taylor series:

$$\begin{aligned}N(j,r,\alpha,\omega,j_0) &= N(j,r,\alpha_0,\omega_0,j_{0,0})\\ &\quad+\left.\frac{\partial N}{\partial j_0}\right|_{j_{0,0}}(j_0-j_{0,0})+\left.\frac{\partial N}{\partial\alpha}\right|_{\alpha_0}(\alpha-\alpha_0)\\ &\quad+\left.\frac{\partial N}{\partial\omega}\right|_{\omega_0}(\omega-\omega_0).\end{aligned}\tag{10}$$

The reason for the first order Taylor series can be known in Ref. [1] and the approximation does not have much influence on the wind precision. After linearization, the equation can be written in matrix form (where numerical subscripts denote channel number) as

$$\begin{pmatrix} N_1 - N_{0,1} \\ \vdots \\ N_{12} - N_{0,12} \end{pmatrix} = \begin{pmatrix} \left.\frac{\partial N_1}{\partial j_0}\right|_{j_{0,0}} & \left.\frac{\partial N_1}{\partial \alpha}\right|_{\alpha_0} & \left.\frac{\partial N_1}{\partial \omega}\right|_{\omega_0} \\ \vdots & \vdots & \vdots \\ \left.\frac{\partial N_{12}}{\partial j_0}\right|_{j_{0,0}} & \left.\frac{\partial N_{12}}{\partial \alpha}\right|_{\alpha_0} & \left.\frac{\partial N_{12}}{\partial \omega}\right|_{\omega_0} \end{pmatrix} \begin{pmatrix} j_0 - j_{0,0} \\ \alpha - \alpha_0 \\ \omega - \omega_0 \end{pmatrix}. \quad (11)$$

The same equation can be written more generally as $\Delta N = G\Delta x$, where G is the generalized matrix to be inverted. The weighted least-square solution to this matrix equation is

$$\Delta x^{\rm est} = (G^{\rm T}WG)^{-1}G^{\rm T}W\Delta N, \quad (12)$$

where $\Delta x^{\rm est}$ is the estimate of Δx, W is a weighting matrix whose diagonal elements are the reciprocal of the signal variance of each channel, and the off-diagonal elements are all zero. Here it is assumed that the signal in each channel is uncorrelated with the signal in any other channel. In fact, there is some slight correlation due to the cross talk between the channels, but this is neglected here. The errors in the model parameters are found from the model covariance matrix:

$$\mathrm{cov}\Delta x = (G^{\rm T}WG)^{-1}, \quad (13)$$

where the statistic error estimates of j_0, α, and ω are already given. The aerosol-molecule ratio can be defined as[3]

$$R = \frac{P_{\rm A}(\pi)\beta_{\rm A}(\pi) + P_{\rm M}(\pi)\beta_{\rm M}(\pi)}{P_{\rm M}(\pi)\beta_{\rm M}(\pi)} = \frac{\alpha + \omega}{\omega}. \quad (14)$$

This ratio expresses the relative aerosol concentration. Figure 2 shows the relationship between the ratio and wavelength. Using propagation of errors, we can express the error in this ratio as

$$\sigma_{\rm R} = \left(\frac{1}{\omega^2}\sigma_\alpha^2 + \frac{\alpha^2}{\omega^4}\sigma_\omega^2 - 2\frac{\alpha}{\omega^3}\sigma_{\alpha\omega}^2\right)^{1/2}, \quad (15)$$

where $\sigma_{\alpha\omega}^2$ is the cross correlation of the aerosol and molecule signals, σ_α^2 is the standard deviation of aerosol signal, σ_ω^2 is the standard deviation of molecule signal. We can acquire the estimates of j_0 and σ_{j_0} by weighted least-square fitting. Wind measurements require knowledge of a zero wind spectral position relative to the measured Doppler-shifted spectra. We collected a reference spectrum at the same time as the atmospheric spectra by collecting light scattered from the outgoing optics. The reference spectrum is assumed to have no Doppler shift. The position of the reference spectrum, $j_{\rm ref,}$ is subtracted from the position of each atmospheric bin and converted to a horizontal wind component in the direction of observation by

$$U_{\rm H} = -\frac{c\Delta\nu_{\rm FSR}\left[j_0(r) - j_{\rm ref}\right]}{2\nu_0 N_{\rm FSR}\sin\phi}. \quad (16)$$

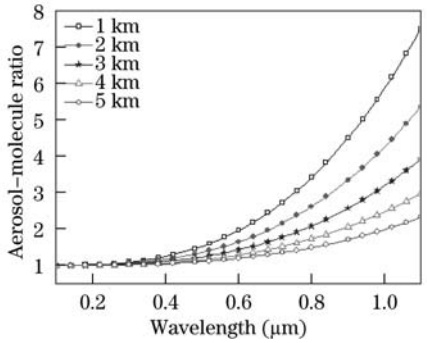

Fig. 2. Aerosol-molecule ratio versus at different altitudes.

The statistic error of wind can be expressed as

$$\sigma_U = \frac{c\Delta\nu_{\rm FSR}}{2\nu_0 N_{\rm FSR}\sin\phi}\left[\sigma_{j_0}^2 + \sigma_{j_{\rm ref}}^2\right]^{1/2}. \quad (17)$$

After neglecting the standard deviation of reference spectrum position, we will discuss the wind error.

The wind error can be attained according to Eq. (17). We choose the parameters in Table 2 for the numerical simulation of wind error at the four wavelengths. The results are shown in Tables 3−5. In order to show the relationship between wind error and altitude at the four different wavelengths of Nd:YAG laser, a comparison is shown in Table 6. It can be seen that the wind error at 1064 nm is the smallest, with the detected energy a little lower than the other three. Through overall consideration of the wind error and the converting efficiency of laser sources, it is sound reasonable to choose the

Table 2. Simulation Parameters for MC Wind Error

Parameter	Value
Transmitted Energy $P_{\rm t}$	60 mJ
Range Bin Length Δh	150 m
Transmission of Optics T_0	5.6%
Plate Reflectivity R	88%
F-P Spacing d	10 cm
Number of Channels $n_{\rm c}$	12
Laser 1/e Width $\Delta\nu_{\rm L}$	0.0045 $\rm cm^{-1}$
Telescope Area $A_{\rm T}$	1555 $\rm cm^2$
Detector Efficiency $Q_{\rm E}$	3.2%
F-P Defect $\Delta d_{\rm D}$	3 nm
Loss Per Plate L	0.2%
FSR $\Delta\nu_{\rm FSR}$	0.049 $\rm cm^{-1}$
Wavelength λ	266,355,532,1064 nm
Molecular 1/e Width $\Delta\nu_{\rm M}$	0.0475 $\rm cm^{-1}$

Table 3. Three Parameters and Wind Error at the Altitude of 2 km

Wavelength (nm)	266	355	532	1064
$\alpha(\times10^{-7}\rm m^{-1})$	1.21504	1.00640	0.753335	0.423038
$\omega(\times10^{-7}\rm m^{-1})$	27.4453	8.65128	1.71533	0.107208
$(\alpha+\omega)/\omega$	1.04427	1.11633	1.43918	4.94595
σ_U(m/s)	0.1584	0.1362	0.1308	0.1246

Table 4. Three Parameters and Wind Error at the Altitude of 3 km

Wavelength (nm)	266	355	532	1064
$\alpha(\times 10^{-8}\mathrm{m}^{-1})$	7.36962	6.10412	4.56921	2.56585
$\omega(\times 10^{-7}\mathrm{m}^{-1})$	24.7903	7.81439	1.54939	0.0968372
$(\alpha+\omega)/\omega$	1.02973	1.07811	1.29490	3.64966
σ_U(m/s)	0.4544	0.4145	0.3447	0.2772

Table 5. Three Parameters and Wind Error at the Altitude of 5 km

Wavelength (nm)	266	355	532	1064
$\alpha(\times 10^{-8}\mathrm{m}^{-1})$	2.71113	2.24558	1.68092	0.943925
$\omega(\times 10^{-7}\mathrm{m}^{-1})$	20.0729	6.32736	1.25455	0.0784096
$(\alpha+\omega)/\omega$	1.01351	1.03549	1.13399	2.20384
σ_U(m/s)	2.5583	2.1570	1.7803	1.118

Table 6. Wind Error Comparison of Four Wavelengths at Different Altitudes

Wavelength (nm)	266	355	532	1064
2-km Altitude	0.1584	0.1362	0.1308	0.1246
3-km Altitude	0.4544	0.4145	0.3447	0.2772
5-km Altitude	2.5583	2.1570	1.7803	1.118

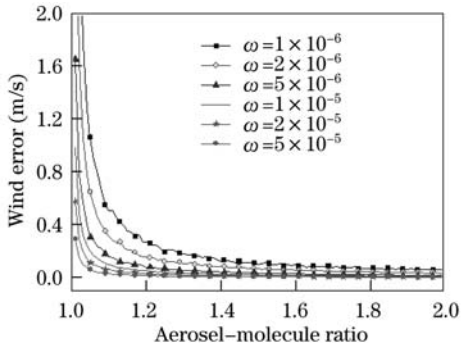

Fig. 3. Wind error versus the aerosol-molecule ratio at different values of ω.

wavelength of 1064 nm as the laser sources for direct-detection Doppler wind lidar. Besides, the relationship between the wind error and the aerosol-molecule ratio is shown in Fig. 3, from with we can find that with the decrease of aerosol-molecule ratio, the statistic error increases notably, especially when the aerosol-molecule ratio is approximately one.

In conclusion, among the four wavelengths for usual Nd:YAG laser, the longer the wavelength is for usual Nd:YAG laser, the higher the aerosol-molecule ratio is. Although the number of received photons decreases, the statistic error for longer wavelength is still the smallest in comparison with the other three due to the greater contribution of the aerosol-molecule ratio. So it is reasonable to choose the wavelength of 1064 nm as the light source of direct-detection Doppler lidar.

This work was supported by the Program of Excellent Team in Harbin Institute of Technology.

References

1. M. J. McGill, W. R. Skinner, and T. D. Irgang, Appl. Opt. **36,** 1253 (1997).
2. M. J. McGill and W. R. Skinner, Opt. Eng. **36,** 139 (1997).
3. M. J. McGill and J. D. Spinhirne, Opt. Eng. **37,** 2675 (1998).
4. D. Morançais, F. Fabre, M. Endemann, and A. Culoma, Proc. SPIE **6750,** 675014 (2007).
5. Y. Ma, H. Lin, H. Ji, and T. Dong, Chinese J. Lasers (in Chinese) **34,** 170 (2007).
6. F. Shen, D. Sun, Z. Zhong, M. Chen, H. Xia, B. Wang, J. Dong, and X. Zhou, Acta Opt. Sin. (in Chinese) **26,** 1761 (2006).
7. X. Cheng, J. Song, F. Li, Y. Dai, and S. Gong, Chinese J. Lasers (in Chinese) **33,** 601 (2006).
8. T. D. Irgang, "Direct-detection Doppler lidar employing a CCD detector: design and early measurements" PhD Thesis (University of Michigan, 2000) p.160.
9. H. Zhang, D. Ren, W. Zhao, Y. Qu, and B. Song, Opto-Electron. Eng. (in Chinese) **35,** (9) 70 (2008).
10. Y. Yuan, D. Ren, and X. Hu, Chin. J. Light Scattering (in Chinese) **17,** 366 (2006).
11. J. Wu, C. Yang, and J. Liu, *Optical Transmission Theory in the Atmosphere* (in Chinese) (Beijing University of Posts and Telecommunications Press, Beijing, 2006) p.11.
12. B. M. Gentry and H. Chen, Proc. SPIE **4893,** 287 (2003).